SEMARAK ILMU PUBLISHING

Journal of Advanced Research in Numerical Heat Transfer

Journal homepage:
https://semarakilmu.com.my/journals/index.php/arnht/index
ISSN: 2735-0142

Analytical Solution for MHD Casson Nanofluid Flow and Heat Transfer due to Stretching Sheet in Porous Medium

Wan Nura'in Nabilah Noranuar[1], Ahmad Qushairi Mohamad[1,*], Lim Yeou Jiann[1], Sharidan Shafie[1], Mohd Anuar Jamaludin[2]

[1] Department of Mathematical Sciences, Faculty of Science, Universiti Teknologi Malaysia, 81310 Johor Bahru, Johor, Malaysia
[2] Department of Mathematics, Universiti Pertahanan Nasional Malaysia, 57000, Kuala Lumpur, Malaysia

ARTICLE INFO

Article history:
Received 20 January 2024
Received in revised form 19 February 2024
Accepted 24 March 2024
Available online 30 April 2024

Keywords:
Casson nanofluid; Stretching sheet; Magnetic field; Porosity; Laplace transformations

ABSTRACT

The feature of having a surface that can stretch has garnered attention in numerous industrial and engineering fields because of its advantages. Nevertheless, most fluid mechanics simulations for stretchable surfaces have predominantly relied on numerical solutions, with a notable lack of theoretical investigations into this matter. Consequently, the current research aims to contribute a theoretical exploration of heat transfer and boundary layer flow for Casson nanofluid on a linearly stretching sheet, considering the existence of porosity and magnetic field effects. Two distinct types of water-based nanofluids containing aluminium oxide and silicon dioxide are examined. By employing similarity transformations, the governing momentum and energy equations undergo transformation and subsequent analytical resolution using Laplace transformations. The resulting solutions are graphically presented to examine the influence of key parameters on temperature and velocity distribution. The analysis indicates that heat transfer is improved by the inclusion of nanoparticles, porosity, and a magnetic field. However, the velocity distribution slows down as a result of higher nanoparticle volume fraction, porosity, and magnetic field imposition.

1. Introduction

Exploring non-Newtonian fluids is a compelling subject for numerous researchers, given its significance in both engineering and industry. The realm of non-Newtonian fluids encompasses issues pertinent to polymer, food processing, petroleum, biomedical field, and chemical industries. Many non-Newtonian fluids are characterised by a nonlinear correlation between stress and strain. Featuring this characteristic, Casson fluid is a non-Newtonian fluid that has a yield stress and requires a certain amount of shear stress to initiate the flow. This model is often used to describe the behavior of certain viscoplastic materials, including various biological fluids like blood and certain food products. Previously, numerous researchers conducted the analysis of boundary layer flow for Casson fluid while considering various aspects such as squeezing Casson fluid flow in channel [1], convective

* *Corresponding author.*
E-mail address: ahmadqushairi@utm.my (Ahmad Qushairi Mohamad)

https://doi.org/10.37934/arnht.19.1.4359

Casson flow over a moving plate [2], Casson fluid flow with heat and mass transfer analysis [3], non-coaxial rotating Casson fluid flow [4], and natural convection flow of Casson fluid in a vertical cylinder [5]. All this research has been studied theoretically, and analytically solved using the Laplace transformations.

The investigation into the Casson fluid flow of the boundary layer coupled with heat transfer along a linearly stretched plate has yielded significant success in recent years, owing to its diverse applications in both scientific research and various industrial processes. Examples of these applications include the processes from various industries like coating and printing, metal spinning, polymer extrusion, continuous stretching plastic films, hot rolling, glass fiber production, and wire drawing. After Sakiadis [6] groundbreaking investigation on the fluid layer flow across both Newtonian and non-Newtonian fluids over a non-linear or linear stretching plate, a vast body of literature has emerged. Furthermore, numerous researchers have extensively examined various aspects of heat transfer and boundary layer flow of Casson fluid analytically related to linear/nonlinear stretching sheets by means of homotopy analysis method [7] and similarity transformations [8,9]. Given the technological applications involved, the nanoparticle impact in Casson fluid flow adjacent to a stretching sheet plays a crucial role in the context of heat transmission attributes. Understanding the heat transfer properties across a stretching plate is vital for achieving the desired quality, as the finished product's value is predominantly dependent on both the stretching rate and heat transfer rate. Nandeppanavar *et al.,* [10] and Alqahtani *et al.,* [11] scrutinized the features of steady Casson nanofluid flow near to exponentially stretching sheet in the presence of heat and mass transmission. Mabood *et al.,* [12] investigated the concept of stretching sheet on radiative boundary layer flow and thermal analysis for Casson nanofluid considering convective boundary condition and variable viscosity. Tawade *et al.,* [13] studied the steady laminar flow of Casson nanofluid across a linearly permeable stretching surface. A different study of Casson nanofluid was conducted by Ullah *et al.,* [14] considering the unsteady flow subjected to a non-linear stretching sheet. Most recently, the concept of stretching sheet in the context of heat transfer and boundary layer flow for Casson nanofluid under various effects can be also referred to the study of Vinita *et al.,* [15], Jain and Kumari [16], and Triveni *et al.,* [17].

Following pioneering study by Andersson *et al.,* [18], numerous researchers were encouraged to extend their investigation into boundary layer flow across a stretching surface for non-Newtonian fluid with the interaction of magnetohydrodynamics (MHD) effects. Amongst them includes Mahabaleshwar *et al.,* [19] performing a viscoelastic fluid flow in the presence of mass diffusion, Hosseinzadeh *et al.,* [20] conducting second grade fluid under the influences of nanoparticles, Patil *et al.,* [21] dealing with a radiative and chemical reacting Williamson nanofluid flow, Bhavana *et al.,* [22] examining Casson fluid flow with mass suction/injection, and Ullah *et al.,* [23] incorporating the effect of porosity and Newtonian heating. All these research [19-23] were investigated numerically using various methods. However, limited study had used the Laplace transformations as the tools to solve this subject analytically. The most related analytical study that used this kind of approach to resolve the MHD flow across stretching surface problem are Ebaid and Al-Sharif [24] and Saleh *et al.,* [25] investigating the consequences of carbon nanotubes (CNTs) nanoparticles for MHD viscous fluid, Maranna *et al.,* [26] investigating the characteristic of heat and mass transfer on MHD Newtonian nanofluid flow, and Sneha *et al.,* [27] scrutinizing radiation and mass transfer effect on MHD CNTs nanofluid flow. In addition, the studies on the impact of porosity in fluid flow contribute to advancements in various fields, ranging from engineering and geophysics to medical and environmental sciences. Amongst those studies performing analytically were Mahabaleshwar *et al.,* [28] considering mass and heat diffusion as well as boundary layer flow for Newtonian fluid in the presence of MHD and porosity. In another study, Mahabaleshwara *et al.,* [29] applied Laplace

transformation to acquire the exact solution for this particular research affected by Navier's slip and chemical reaction. Considering the model of Casson fluid, Wahid *et al.,* [30] analytically investigated thermal analysis and MHD radiative boundary layer flow in a porous medium across a linearly stretching sheet.

According to the above-mentioned literature, due to the complex nature of the stretching sheet study, most researchers conducted the investigation numerically and limited analytical study was reported, especially using Laplace transformation as the method of solutions. To be more clearer, no study has been conducted for the application of Laplace transformations as the method to solve the Casson nanofluid flow bounded with a linearly stretching sheet. Therefore, inspired by this gap of study, this present work focused on the impacts of MHD and porosity, and the novelty is to generate the exact solution via Laplace transformations for MHD Casson nanofluid flow with heat transfer saturated in porous medium through a stretching sheet. The derived ordinary differential equations (ODEs) are acquired through the transformation of partial differential equations (PDEs) using appropriate variables. Analytical outcomes can be achieved by employing various controlling parameters. The temperature equation can be analytically explored and expressed in terms of incomplete gamma functions. Results can be attained through the utilization of diverse physical parameters. The conclusion drawn was that using the Laplace transform for solving leads to simpler special functions, while alternative methods, as demonstrated by Saeed *et al.,* [7] and Wahid *et al.,* [30], yield more intricate special functions. Hence, this transformation is a popular computational tool in engineering problems and provides a systematic alternative approach to solve differential equations by simplifying the solution of problems.

2. Mathematical Formulation

The study considers an incompressible steady flow of MHD Casson nanofluid over a sheet saturated in porous medium, as illustrated in Figure 1. The sheet undergoes a horizontally linearly stretched along x-axis with the velocity $u = ax$ where a is a constant. The sheet is positioned at $y = 0$, where y-axis is taken in upward direction. A uniform magnetic field B_0 is applied transversely toward normal of the stretching sheet. The Casson nanofluid, composed of water base fluid incorporates various metal oxide nanoparticles (Al_2O_3 and SiO_2) [31, 32]. The study assumes no slip between the base fluid and the nanoparticles, and both are in thermal equilibrium.

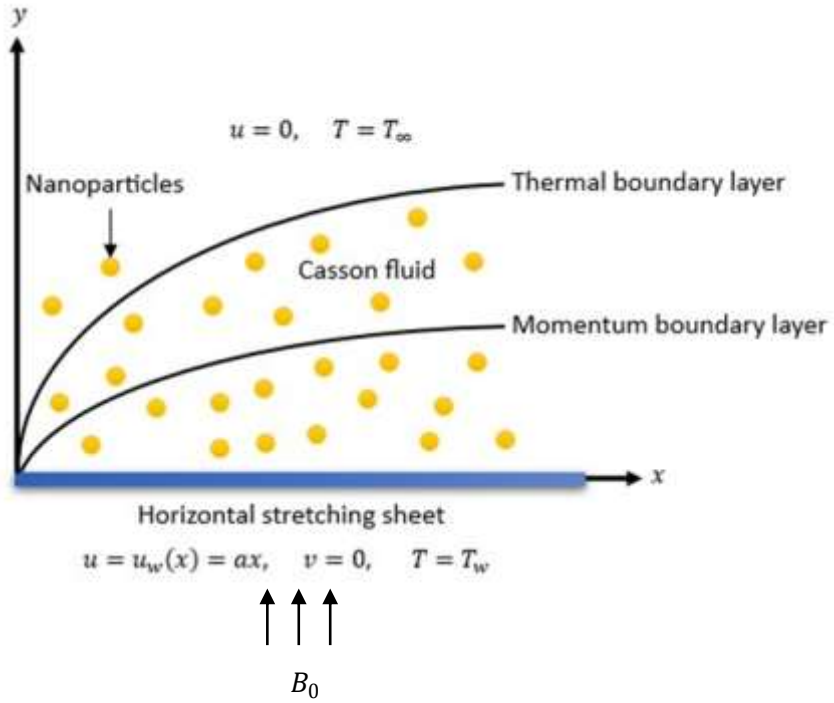

Fig. 1. Physical geometry of the flow

The rheological equations describe the flow behavior of fluids, which are essential in understanding the material deformation and flow under different conditions. Non-Newtonian fluids exhibit more complex flow behaviors, and different rheological equations are used to describe their behavior. For an incompressible Casson fluid flow, the rheological equation is expressed by following stress tensor [4, 5]:

$$\tau_{ij} = \begin{cases} \left(\mu_b + \frac{\tau_y}{\sqrt{2\pi}}\right) 2e_{ij}\pi > \pi_c, \\ \left(\mu_b + \frac{\tau_y}{\sqrt{2\pi}}\right) 2e_{ij}\pi < \pi_c. \end{cases} \tag{1}$$

In the above correlation (1), τ_y and μ_b are the yield stress and plastic dynamic, $\pi = e_{ij}e_{ij}$, with e_{ij} is the $(i,j)^{th}$ element of the deformation rate and π_c is the critical value of the deformation rate. Under this assumption and adapting Tiwari and Das model [33], the momentum and energy equations are written as

$$\frac{\partial u}{\partial x} + \frac{\partial v}{\partial y} = 0, \tag{2}$$

$$u\frac{\partial u}{\partial x} + v\frac{\partial u}{\partial y} = \nu_{nf}\left(1 + \frac{1}{\beta}\right)\frac{\partial^2 u}{\partial y^2} - \frac{\sigma_{nf}B_o^2 u}{\rho_{nf}} - \frac{\nu_{nf}}{k}u, \tag{3}$$

$$\left(\rho C_p\right)_{nf}\left(u\frac{\partial T}{\partial x} + v\frac{\partial T}{\partial y}\right) = k_{nf}\frac{\partial^2 T}{\partial y^2}. \tag{4}$$

with the initial and boundary conditions

$$u = u_w(x) = ax,\ v = 0; \quad T = T_w; \quad y = 0, \tag{5}$$

$$u = 0; \quad T = T_\infty; \quad y \to \infty. \tag{6}$$

In the above equations, u and v are the x and y direction of velocity components, respectively, T is the temperature of nanofluid, and $\beta = {\mu\sqrt{2\pi_c}}/{\tau_y}$ is Casson fluid parameter, a is a positive stretching rate constant and the ambient temperature T_∞ represents the temperature aways from stretching surface, while the constant T_w represents the temperature at the stretching surface. The nanofluid correlation by Tiwari and Das [33] are expressed in Table 1, where the subscript nf, f, and s are nanofluid, base fluid, and nanoparticles, and ϕ is the volume fraction of nanoparticle. Table 2 displays the thermal physical characteristics for the base fluids and nanoparticles.

By configuring the following similarity variables, Eq. (2) is immediately met,

$$u = axf'(\eta), \quad v = -\sqrt{av}f(\eta), \quad \eta = \sqrt{\frac{a}{v}}y, \quad \theta(\eta) = \frac{T - T_\infty}{T_w - T_\infty}, \tag{7}$$

and, Eq. (3) and Eq. (4) take the form

$$\left(1 + \frac{1}{\beta}\right)f'''(\eta) + \phi_1[f(\eta)f''(\eta) - f(\eta)'^2] - [\phi_2 M + \phi_1 K]f'(\eta) = 0, \tag{8}$$

$$\tau\theta''(\eta) + f(\eta)\theta'(\eta) = 0, \tag{9}$$

where

$$\begin{gathered}\phi_1 = (1-\phi)^{2.5}\left[1 - \phi + \phi\left(\frac{\rho_s}{\rho_f}\right)\right], \quad \phi_2 = (1-\phi)^{2.5}\left[1 + \frac{3(\sigma-1)\phi}{\sigma + 2 - (\sigma-1)\phi}\right], \\ \sigma = \frac{\sigma_s}{\sigma_f}, \quad \tau = \frac{1}{Pr}\left(\frac{k_{nf}}{k_f}\right)\left(\frac{1}{\left(1 - \phi + \phi\left(\frac{\rho_s}{\rho_f}\right)\right)}\right),\end{gathered} \tag{10}$$

are nanofluid constants and

$$\mathrm{Pr} = \frac{\left(\rho C_p\right)_f \nu_f}{k_f}, \quad M = \frac{\sigma_f B_0^2 a^2}{\rho_f \nu_f}, \quad K = \frac{\nu_f}{ka}, \tag{11}$$

are Prandtl number, magnetic field, and porosity.

Table 1
Nanofluid correlation by Tiwari and Das model [33]

Properties	Nanofluid correlation
Kinematic viscosity, ν	$\nu_{nf} = \frac{\mu_{nf}}{\rho_{nf}}$
Dynamic viscosity, μ	$\mu_{nf} = \frac{\mu_f}{(1-\phi)^{2.5}}$
Density, ρ	$\rho_{nf} = (1-\phi)\rho_{nf} + \phi\rho_s$
Specific heat capacitance, C_p	$(C_p)_{nf} = \frac{(1-\phi)(\rho C_p)_f + (\rho C_p)_s}{\rho_{nf}}$
Thermal conductivity, k	$k_{nf} = k_f \left\{ \frac{k_s + 2k_f - 2\phi(k_f - k_s)}{k_s + 2k_f + 2\phi(k_f - k_s)} \right\}$
Electrical conductivity, σ	$\sigma_{nf} = \sigma_f \left\{ 1 + \frac{3\left(\frac{\sigma_s}{\sigma_f} - 1\right)\phi}{\left(\frac{\sigma_s}{\sigma_f} + 2\right) - \phi\left(\frac{\sigma_s}{\sigma_f} - 1\right)} \right\}$

Table 2
Characteristics of thermal physical for water and considered nanoparticles [31, 32]

Base fluid / nanoparticles	Water	Al_2O_3	SiO_2
$\rho(Kgm^{-3})$	996.5	3970	2650
$C_p(JKg^{-1}K^{-1})$	4181	765	730
$k(Wm^{-1}K\text{^}-1)$	0.613	40	1.5
$\sigma(Sm^{-1})$	5.5 ×10^{-6}	35 ×10^{6}	0.0005

The transformed boundary conditions for stretching sheet case are

$$f(\eta) = 0, \quad f'(\eta) = 1, \quad \theta(\eta) = 1; \quad \eta = 0, \tag{12}$$

$$f'(\eta) = 1, \quad \theta(\eta) = 0; \quad \eta \to \infty. \tag{13}$$

where f and θ are the dimensionless stream function and temperature function, respectively, and the prime denotes differentiation with respect to η.

3. Exact Solutions

3.1 Velocity Distribution

As according to Saleh *et al.,* [25], the boundary layer flow for Eq. (8) possesses the exact solution which can be presented in the exponential type

$$f(\eta) = A_1 + A_2 \exp(-c\eta), \tag{14}$$

where A_1 and A_2 are the constant obtained as

$$A_1 = \frac{1}{c}, \quad A_2 = -\frac{1}{c}. \tag{15}$$

Eq. (8) incorporates Eq. (14) and Eq. (15), the relation of constant c in Eq. (15) is found as

$$c = \sqrt{\frac{(\phi_1 + \phi_2 M + \phi_1 K)\beta}{\beta + 1}}, \tag{16}$$

and the velocity distribution is determined to be

$$f'(\eta) = \exp(-c\eta). \tag{17}$$

3.2 Temperature Distribution

For thermal transport, incorporating Eq. (14) and Eq. (15) into Eq. (9) yields

$$\tau\theta''(\eta) + \left(\frac{1}{c} - \frac{1}{c}\exp(-c\eta)\right)\theta'(\eta) = 0. \tag{18}$$

Next, Eq. (18) is transformed using the independent variable $t = \exp(-c\eta)$ [25] to become

$$t\theta''(t) + (r - st)\theta'(t) = 0, \tag{19}$$

where $r = 1 - {}^{1}/_{\tau c^2}$ and $s = -{}^{1}/_{\tau c^2}$ are constants, and subjected to the conditions

$$\theta(0) = 0, \quad \theta(1) = 1. \tag{20}$$

Then, Eq. (19) is employed with the Laplace transform, leads to

$$q(r - q)\Theta(q) + [r + (s - 2)q]\Theta(q) = 0, \tag{21}$$

where $\Theta(q)$ is the Laplace transform of $\theta(t)$. After that, Eq. (21) is integrated to become

$$\Theta(q) = \frac{m}{q(q - r)^{1-s}}, \tag{22}$$

where m is an integration constant. Imposing Eq. (22) with the inverse Laplace transform gives

$$\theta(t) = \frac{m}{\Gamma(1 - s)}(t^{-s}\exp(rt)), \quad s < 1, \tag{23}$$

which fulfilled the boundary $\theta(0) = 0$ automatically. In accordance with the convolution property details described in Saleh *et al.,* [25], Eq. (23) turns into

$$\theta(t) = \frac{m}{\Gamma(1 - s)}\left(-\frac{1}{r}\right)^{1-s}\Gamma(1 - s, 0, -rt). \tag{24}$$

By applying the other boundary condition $\theta(1) = 1$, m is obtained as

$$m = \frac{\Gamma(1-s)}{\left(-\frac{1}{r}\right)^{1-s}\Gamma(1-s,0,-r)}. \tag{25}$$

Consequently, following is the exact solution for $\theta(t)$ in the form of generalized gamma function

$$\theta(t) = \frac{\Gamma(1-s,0,-rt)}{\Gamma(1-s,0,-r)}, \tag{26}$$

and the term of η for Eq. (26) is expressed as

$$\theta(\eta) = \frac{\Gamma(1-s,0,-re^{-c\eta})}{\Gamma(1-s,0,-r)}. \tag{27}$$

4. Results and Discussion

The primary objective of this section is to examine the ways of dimensionless constraints affect their corresponding profiles. The reduced ordinary differential equations (ODEs), Eq. (9) and Eq. (10) subjected to the boundaries (13) and (14) are solved analytically to acquire the solutions for velocity and temperature distributions. The obtained solutions are visually represented through the utilization of MATLAB software, and their characteristics are further scrutinized through an in-depth discussion. The analysis for velocity and temperature profiles are influenced by significant parameters on Casson fluid, porosity, magnetic field, nanoparticle volume fraction, and Prandtl number, which are varied within the range of $0.5 \leq \beta \leq 2$, $2 \leq K \leq 8$, $2 \leq M \leq 8$, $0.01 \leq \phi \leq 0.04$, and $1 \leq \mathrm{Pr} \leq 6.2$ [8, 10, 34]. All the computational in this study involves the dispersion of water based Al_2O_3 and water based SiO_2 with their thermophysical characteristics is referred in Table 1.

4.1 Results Validation

The validation of the present results with the existing published study by Bhattacharyya *et al.,* [9] is depicted in Figure 2. In the study of Bhattacharyya *et al.,* [9], the steady flow of Casson fluid over a linearly stretching sheet is investigated while incorporating the suction effect. An extension to this study is performed by introducing other effects such as nanoparticles, magnetic field, and porosity effects. The comparison of both study is carried out by setting the numerical value for suction parameter, $S = 0$ in the published study by Bhattacharyya *et al.,* [9] and setting the following parameters' value $\phi = M = K = 0$ in the present study. This approach is known as limiting cases, where setting up the certain parameter value to 0 is purposely to reduce both problems to an identical case. A good limiting case should provide results that closely match observations. For this study, the findings are observed to be in excellent agreement, where both studies lie on the identical profile.

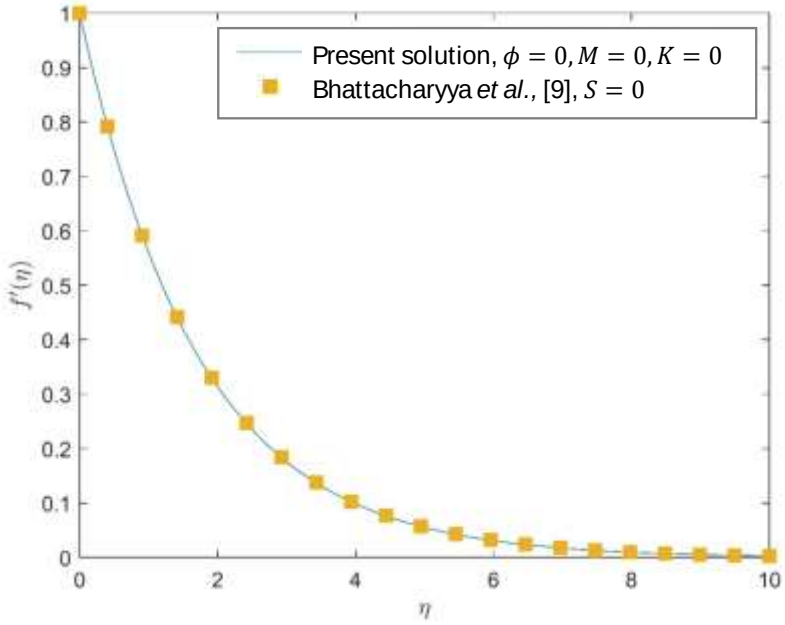

Fig. 2. Validation of present results

4.2 Velocity Distribution

Figure 3 presents the outcomes of a magnetic constraint (M), revealing that an increase in the magnetic field results in a reduction of the velocity field for both nanofluids. However, the electric field, characterized by an accelerating force, leads to an elevation of the velocity field near the stretching sheet. The Lorentz force, on the other hand, functions to impede motion, thereby increasing the mechanical resistance to both Al_2O_3 and SiO_2 nanofluid motion within the momentum boundary layer width. Consequently, this enlarges the speed differential of nanofluids at the surface. To verify this finding, Aloliga *et al.*, [8] and Ebaid and Al-Sharif [24] also reported the similar results of MHD effect on non-Newtonian fluid flow.

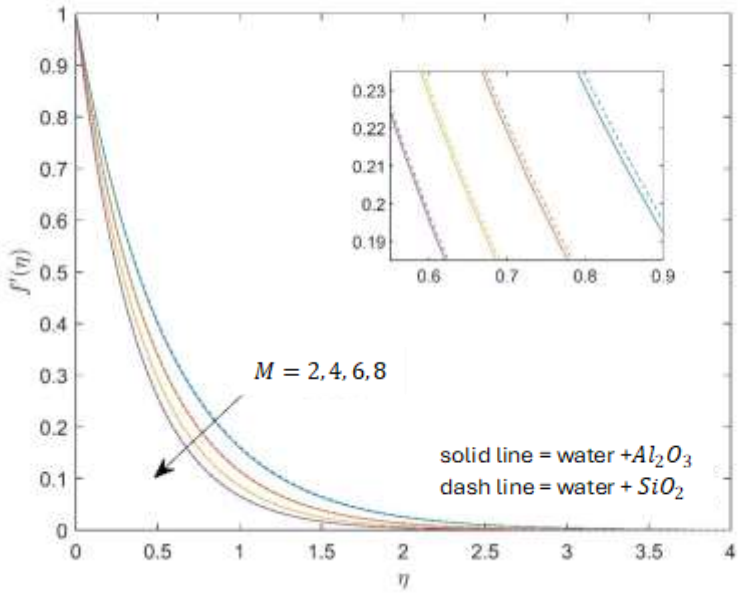

Fig. 3. Impact of M on $f'(\eta)$

Figure 4 depicts alterations in the velocity profile associated with the Casson fluid constraint (β). When Casson fluid constraint augments, the fluid velocity of water-Al_2O_3 and water-SiO_2 nanofluids decreases. Simultaneously, viscosity increases due to yield stress, which acts in opposition to the fluid's movement within the layer closest to the boundary. In Figure 5, the influence of porous media constraint (K) on both velocity dispersion is demonstrated. As K undergoes escalation, the velocity profile in the flow direction decreases. In practical terms, elevated values of the porous parameter signify heightened viscous forces, resulting in a prevalence of inertial forces, thereby causing a reduction in velocity. The results of enhancement β and K values can be verified by the study of Nandeppanavar et a. [10], where this study also observed the same effect on velocity profile.

Figure 6 demonstrates the impacts of nanoparticle volume fraction constraint (ϕ), exhibiting a decreasing velocity profile of water-Al_2O_3 nanofluid with greater volume fraction of nanoparticles, which also found in the study of Krishna [35]. Theoretically, nanoparticles often contribute to higher viscosity in the fluid. In this case, the rise volume fraction nanoparticles cause the fluid to become more viscous, which tends to impede the fluid flow, resulting in a decrease in velocity. However, the water-SiO_2 nanofluid experiences an opposite velocity effect to water-Al_2O_3 nanofluid, which is increasing velocity profile is reported. This profile's behavior may be affected by a decreased viscosity of water-SiO_2 nanofluid when the nanoparticles are added more in water. Lower viscosity can facilitate smoother fluid flow, contributing to an increase in the velocity profile.

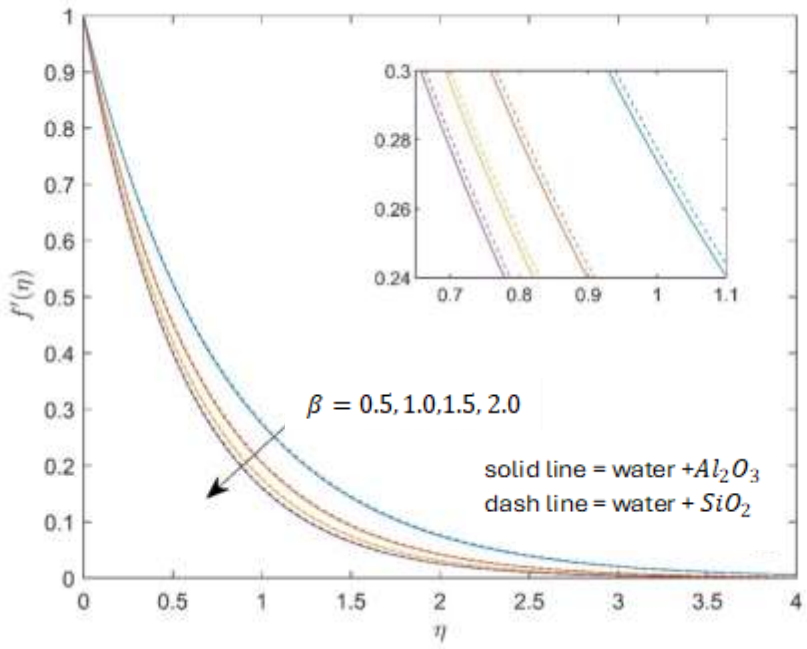

Fig. 4. Impact of β on $f'(\eta)$

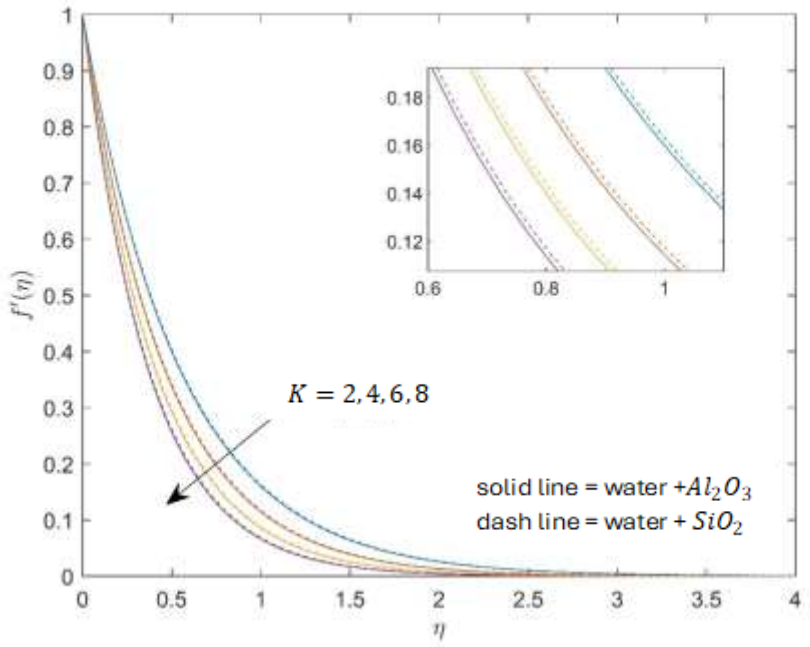

Fig. 5. Impact of K on $f'(\eta)$

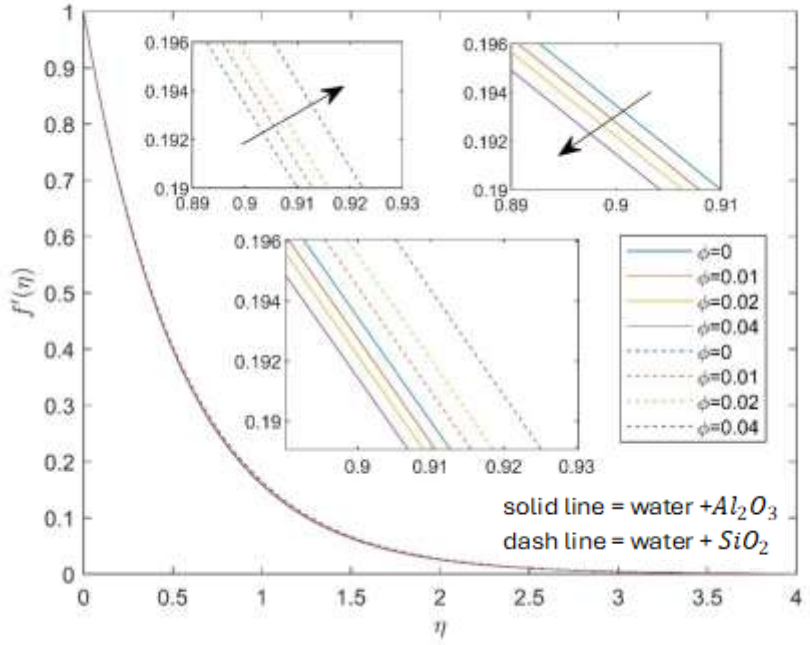

Fig. 6. Impact of ϕ on $f'(\eta)$

4.3 Temperature Distribution

Figure 7 illustrates the impact of magnetic constraint (M) on the temperature profile for both nanofluids. Larger magnetic constraints result in an increase in the width of the thermal boundary layer. The heightened Lorentz force within the magnetic field, indicated by higher M values, contributes to the expansion of the temperature boundary layer. The existence of a magnetic field results in the emergence of a resistive force referred to as the Lorentz force, effectively reducing the

fluid's velocity, and causing a diminution in the width of boundary layer flow. Additionally, an escalation in the thermal gradient led to an observed enlargement in the width of the temperature boundary layer.

Figure 8 presents the perspective of β on both nanofluids' temperature distribution. Higher values of the Casson constraint (β) contribute to an increase in thermal distribution. The impacts of the Casson fluid constraint result in elevated temperatures within the boundary layer and a reduction in yield stress. The Casson liquid is characterized by variable plastic dynamic viscosity and a pronounced impact of yield stress. With an increase in the Casson fluid constraint, there is an increase in velocity near the wall, with a slight decrease further away from the wall. Figure 9 shows that the temperature gains of both nanofluids with the effect of porosity K. Higher medium porosity often means a larger volume of void spaces within the medium. This increased porosity allows for better fluid flow and improved heat transfer. Consequently, fluid temperature within the porous medium rises. Ullah *et al.,* [23] report similar β and K impacts on temperature profiles, hence verifying the current findings.

Figure 10 depicts the temperature distribution affected by the nanoparticle volume fraction ϕ. An upsurge of ϕ increases the temperature distribution, which is also reported by Ebaid and Al-Sharif [24] and Ahmad *et al.,* [31]. Nanoparticles often have higher thermal conductivity compared to the base fluid. As the volume fraction of both types of nanoparticles increases, the overall thermal conductivity of the nanofluid improves, enhancing the ability of the nanofluid to absorb heat. This can result in better heat transport and rise of thermal profile. Figure 11 elucidates the behavior of temperature gradients for various Pr values. The figure indicates that an increase in Pr leads to a decrease in temperature profiles, resulting in a reduction in the width of the thermal boundary layer. This suggests that with an increase in Pr, heat diffuses more rapidly. Consequently, as Pr rises, the heat diffusivity of the fluid increases, leading to a rapid heat loss and reduce temperature accordingly. This current finding of M and Pr can be verified by Aloliga *et al.,* [8].

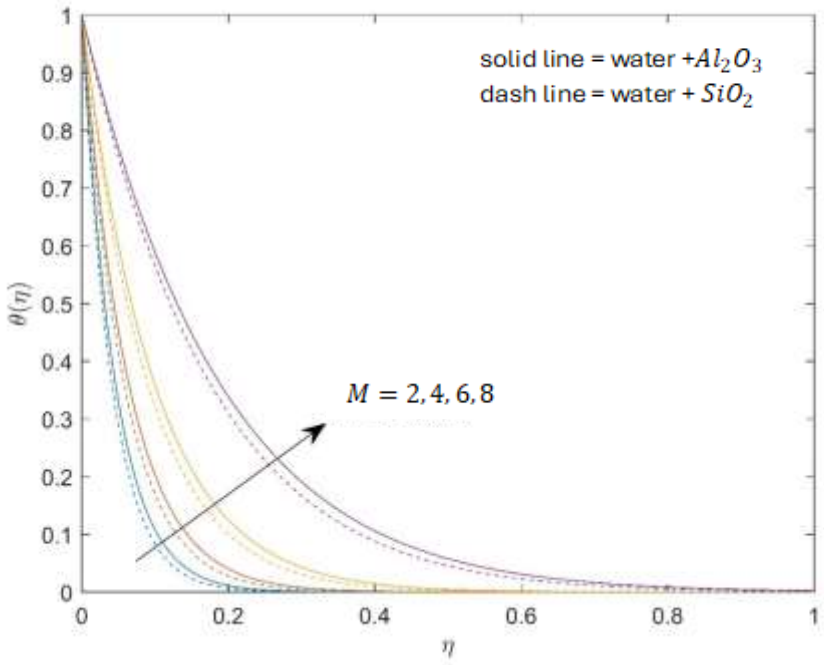

Fig. 7. Impact of M on $\theta(\eta)$

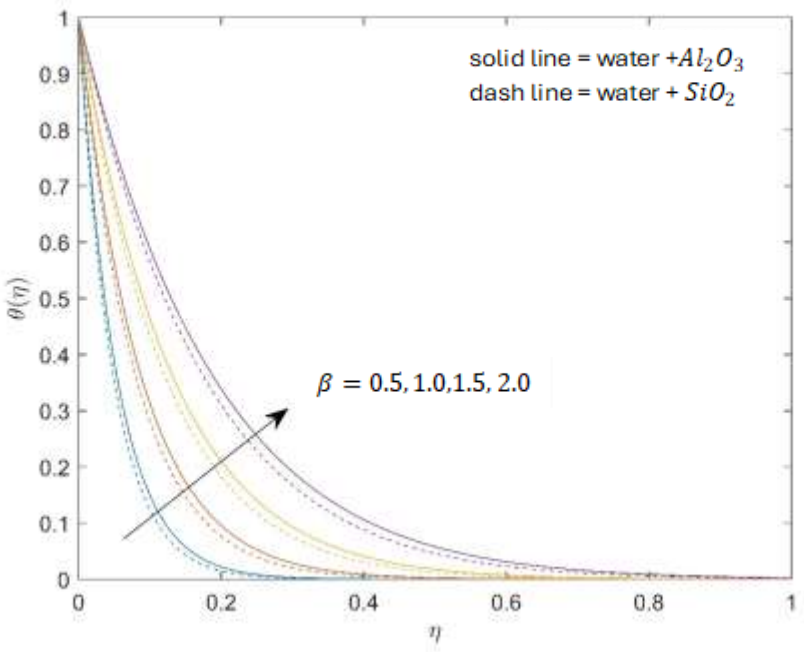

Fig. 8. Impact of β on $\theta(\eta)$

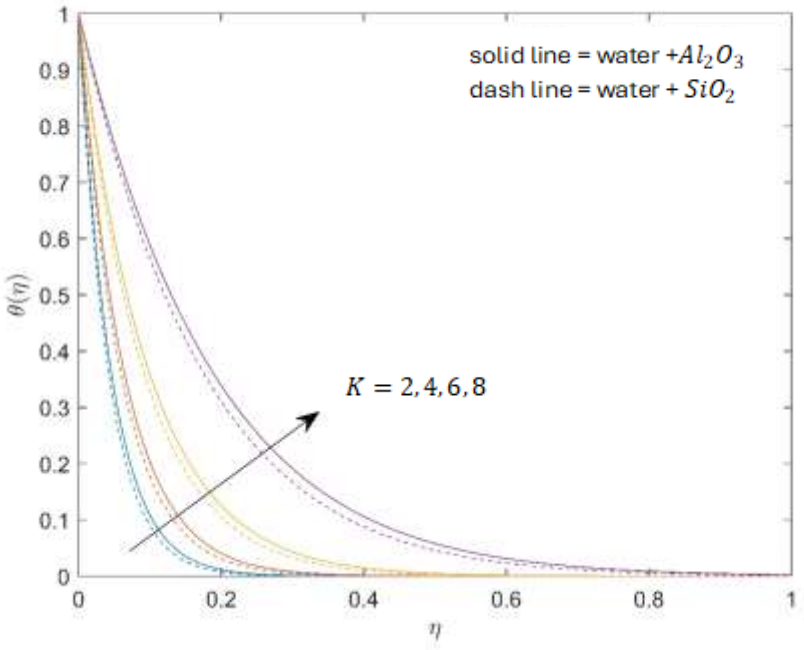

Fig. 9. Impact of K on $\theta(\eta)$

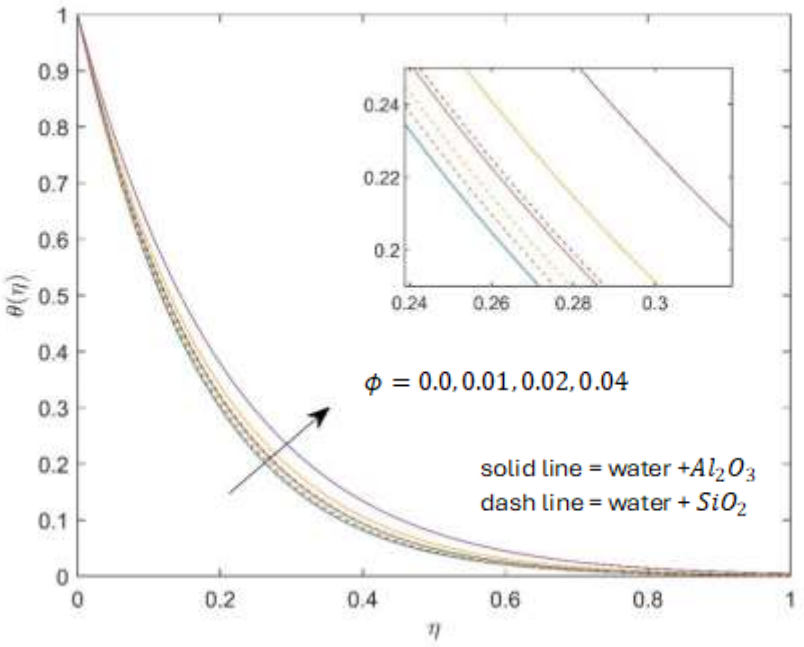

Fig. 10. Impact of ϕ on $\theta(\eta)$

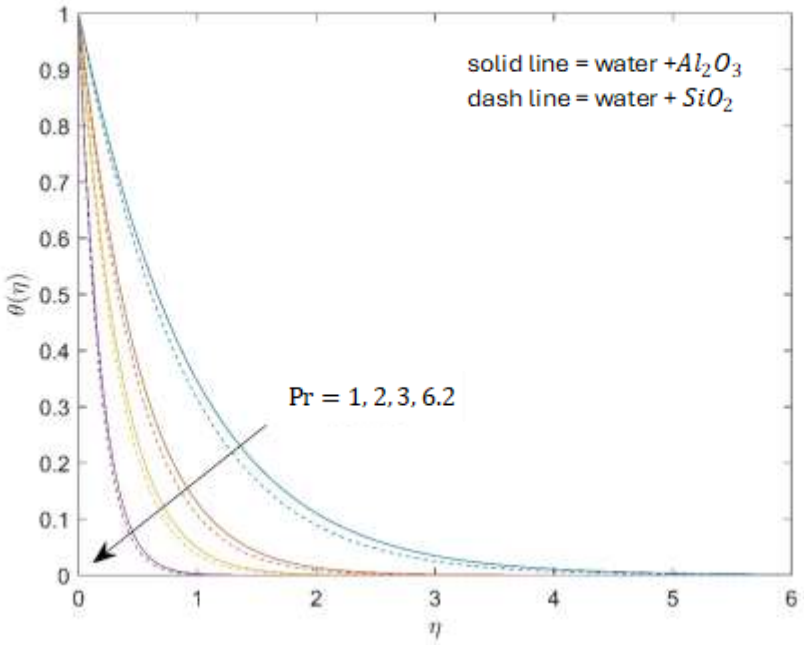

Fig. 11. Impact of Pr on $\theta(\eta)$

4.4 Comparison of Water Based Al_2O_3 and Water Based SiO_2

For the case of velocity profile, a prominent effect of water based SiO_2 nanofluid is observed compared to water based Al_2O_3 nanofluid. It is noteworthy that the density ratio of nanoparticles to the fluid significantly influences the viscosity. This is supported by the correlation established by Machrafi [36], where the density of nanoparticles and fluids have a direct relation with the viscosity of nanofluid. In this case, the prominent velocity effect of water based SiO_2 nanofluid is due to the

low density of SiO_2 nanoparticles. Meanwhile, for the case of temperature profile, water-Al_2O_3 nanofluid experiences higher magnitude compared to water-SiO_2 nanofluid. The temperature difference between both nanofluids can be influenced by their nanofluid thermal conductivity. It is important to note that the ability of heat conduction and heat transfer for nanofluid is significantly influenced by the thermal conductivity. In this case, thermal conductivity for water-Al_2O_3 nanofluid is superior to water-SiO_2 nanofluid, leading to more conduction of heat by the water-Al_2O_3 nanofluid and consequently increase the temperature profile.

5. Conclusions

This study addresses a cost-effective analytical simulation for a two-dimensional, incompressible, and steady forced convective Casson nanofluid flow towards a linearly stretching sheet. An applied magnetic field is imposed to fluid flow that has been saturated in a porous medium. The analysis includes an examination of heat transport, considering magnetohydrodynamics and porosity effects. The obtained results are validated against existing theoretical data from Bhattacharyya *et al.,* [9], showing good agreement with the present computational analysis. To explore the behavior of the proposed problem over a stretched surface, the study discusses the graphical impacts of Casson parameter, magnetic field, porosity, and nanoparticle volume fraction in the presence of both alumina and silicon dioxide in water. The analysis concludes with meaningful final remarks as follows:

i. An elevation velocity profile is observed for increasing values of M, β, and K.
ii. For increasing values of ϕ, water-Al_2O_3 nanofluid experiences an enhancement velocity profile while water-SiO_2 nanofluid experiences a reduction velocity profile.
iii. An enhancement temperature profile is observed for increasing values of M, β, K, and ϕ.
iv. A temperature drop is observed for increasing Pr values.
v. For velocity profiles, water-SiO_2 nanofluid has higher magnitude compared to water-Al_2O_3 nanofluid due to lower density property by SiO_2 nanoparticles.
vi. For temperature profiles, water-Al_2O_3 nanofluid has higher magnitude compared to water-SiO_2 nanofluid due to high thermal conductivity property by Al_2O_3 nanoparticles.

Acknowledgement
This research was funded by Universiti Teknologi Malaysia under Matching Grant Scheme R.J130000.7354.4B748 and Q.J130000.3054.03M77.

References
[1] Qayyum, Mubashir, Efaza Ahmad, Sidra Afzal, Tanveer Sajid, Wasim Jamshed, Awad Musa, El Sayed M. Tag El Din, and Amjad Iqbal. "Fractional analysis of unsteady squeezing flow of Casson fluid via homotopy perturbation method." *Scientific Reports* 12, no. 1 (2022): 18406. https://doi.org/10.1038/s41598-022-23239-0
[2] Khan, Dolat, Arshad Khan, Ilyas Khan, Farhad Ali, Faizan ul Karim, and I. Tlili. "Effects of relative magnetic field, chemical reaction, heat generation and Newtonian heating on convection flow of Casson fluid over a moving vertical plate embedded in a porous medium." *Scientific reports* 9, no. 1 (2019): 400. https://doi.org/10.1038/s41598-018-36243-0
[3] Abbas, Shajar, Zaib Un Nisa, Mudassar Nazar, Muhammad Amjad, Haider Ali, and Ahmed Zubair Jan. "Application of heat and mass transfer to convective flow of casson fluids in a microchannel with Caputo–Fabrizio derivative approach." *Arabian Journal for Science and Engineering* (2023): 1-12. https://doi.org/10.1007/s13369-023-08351-1
[4] Noranuar, Wan Nura'in Nabilah, Ahmad Qushairi Mohamad, Sharidan Shafie, Ilyas Khan, Lim Yeou Jiann, and Mohd Rijal Ilias. "Non-coaxial rotation flow of MHD Casson nanofluid carbon nanotubes past a moving disk with porosity effect." *Ain Shams Engineering Journal* 12, no. 4 (2021): 4099-4110. https://doi.org/10.1016/j.asej.2021.03.011

[5] Azmi, Wan Faezah Wan, Ahmad Qushairi Mohamad, Lim Yeou Jiann, and Sharidan Shafie. "Unsteady natural convection flow of blood Casson nanofluid (Au) in a cylinder: nano-cryosurgery applications." *Scientific reports* 13, no. 1 (2023): 5799. https://doi.org/10.1038/s41598-023-30129-6

[6] Sakiadis, B. C. "Boundary-layer behavior on continuous solid surfaces: II. The boundary layer on a continuous flat surface." *AiChE journal* 7, no. 2 (1961): 221-225. https://doi.org/10.1002/aic.690070211

[7] Saeed, Anwar, Ebrahem A. Algehyne, Musaad S. Aldhabani, Abdullah Dawar, Poom Kumam, and Wiyada Kumam. "Mixed convective flow of a magnetohydrodynamic Casson fluid through a permeable stretching sheet with first-order chemical reaction." *Plos one* 17, no. 4 (2022): e0265238. https://doi.org/10.1371/journal.pone.0265238

[8] Aloliga, Golbert, Yakubu Ibrahim Seini, and Rabiu Musah. "Heat transfer in a magnetohydrodynamic boundary layer flow of a non-newtonian casson fluid over an exponentially stretching magnetized surface." *Journal of Nanofluids* 10, no. 2 (2021): 172-185. https://doi.org/10.1166/jon.2021.1777

[9] Bhattacharyya, Krishnendu, Tasawar Hayat, and Ahmed Alsaedi. "Exact solution for boundary layer flow of Casson fluid over a permeable stretching/shrinking sheet." *ZAMM-Journal of Applied Mathematics and Mechanics/Zeitschrift für Angewandte Mathematik und Mechanik* 94, no. 6 (2014): 522-528. https://doi.org/10.1002/zamm.201200031

[10] Nandeppanavar, Mahantesh M., S. Vaishali, M. C. Kemparaju, and N. Raveendra. "Theoretical analysis of thermal characteristics of casson nano fluid flow past an exponential stretching sheet in Darcy porous media." *Case Studies in Thermal Engineering* 21 (2020): 100717. https://doi.org/10.1016/j.csite.2020.100717

[11] Alqahtani, Aisha M., Muhammad Bilal, Muhammad Usman, Theyab R. Alsenani, Aatif Ali, and Samy Refahy Mahmuod. "Heat and mass transfer through MHD Darcy Forchheimer Casson hybrid nanofluid flow across an exponential stretching sheet." *ZAMM-Journal of Applied Mathematics and Mechanics/Zeitschrift für Angewandte Mathematik und Mechanik* (2023): e202200213. https://doi.org/10.1002/zamm.202200213

[12] Mabood, F., S. M. Ibrahim, P. V. Kumar, and G. Lorenzini. "Effects of slip and radiation on convective MHD Casson nanofluid flow over a stretching sheet influenced by variable viscosity." *Journal of Engineering Thermophysics* 29 (2020): 303-315. https://doi.org/10.1134/S1810232820020125

[13] Tawade, Jagadish V., C. N. Guled, Samad Noeiaghdam, Unai Fernandez-Gamiz, Vediyappan Govindan, and Sundarappan Balamuralitharan. "Effects of thermophoresis and Brownian motion for thermal and chemically reacting Casson nanofluid flow over a linearly stretching sheet." *Results in Engineering* 15 (2022): 100448. https://doi.org/10.1016/j.rineng.2022.100448

[14] Ullah, Imran, Kottakkaran Sooppy Nisar, Sharidan Shafie, Ilyas Khan, Muhammad Qasim, and Arshad Khan. "Unsteady free convection flow of casson nanofluid over a nonlinear stretching sheet." *IEEE Access* 7 (2019): 93076-93087. https://doi.org/10.1109/ACCESS.2019.2920243

[15] Makkar, Vinita, Vikas Poply, and Naresh Sharma. "Three Dimensional Modelling of Magnetohydrodynamic Bio-Convective Casson Nanofluid Flow with Buoyancy Effects Over Exponential Stretching Sheet Along with Heat Source & Gyrotactic Micro-Organisms." *Journal of Nanofluids* 12, no. 2 (2023): 535-547. https://doi.org/10.1166/jon.2023.1921

[16] Jain, Shalini, and Ranjana Kumari. "Analysis of Casson Nanofluid Flow and Heat Transfer Across a Non-linear Stretching Sheet Adopting Keller Box Finite Difference Scheme." *International Journal of Applied and Computational Mathematics* 9, no. 6 (2023): 134. https://doi.org/10.1007/s40819-023-01619-y

[17] Triveni, Battena, Munagala Venkata Subba Rao, Kotha Gangadhar, and Ali J. Chamkha. "Heat transfer analysis of MHD Casson nanofluid flow over a nonlinear stretching sheet in the presence of nonuniform heat source." *Numerical Heat Transfer, Part A: Applications* (2023): 1-20. https://doi.org/10.1080/10407782.2023.2219831

[18] Andersson, H. I., K. H. Bech, and B. S. Dandapat. "Magnetohydrodynamic flow of a power-law fluid over a stretching sheet." *International Journal of Non-Linear Mechanics* 27, no. 6 (1992): 929-936. https://doi.org/10.1016/0020-7462(92)90045-9

[19] Mahabaleshwar, Ulavathi Shettar, Thippeswamy Anusha, David Laroze, Nejla Mahjoub Said, and Mohsen Sharifpur. "An MHD flow of non-Newtonian fluid due to a porous stretching/shrinking sheet with mass transfer." *Sustainability* 14, no. 12 (2022): 7020. https://doi.org/10.3390/su14127020

[20] Hosseinzadeh, Kh, M. R. Mardani, M. Paikar, A. Hasibi, T. Tavangar, M. Nimafar, D. D. Ganji, and M. B. Shafii. "Investigation of second grade viscoelastic non-Newtonian nanofluid flow on the curve stretching surface in presence of MHD, Results in Engineering 17 (2023), 100838." (2022). https://doi.org/10.1016/j.rineng.2022.100838

[21] Patil, Vishwambhar S., Pooja P. Humane, and Amar B. Patil. "MHD Williamson nanofluid flow past a permeable stretching sheet with thermal radiation and chemical reaction." *International Journal of Modelling and Simulation* 43, no. 3 (2023): 185-199. https://doi.org/10.1080/02286203.2022.2062166

[22] Bhavana, P. M., G. P. Vanitha, U. S. Mahabaleshwar, and Basma Souayeh. "Effect of magnetohydrodynamic Casson fluid flow on the stretching/shrinking surface." *ZAMM-Journal of Applied Mathematics and Mechanics/Zeitschrift für Angewandte Mathematik und Mechanik* (2023): e202200523. https://doi.org/10.1002/zamm.202200523

[23] Ullah, Imran, Sharidan Shafie, and Ilyas Khan. "Effects of slip condition and Newtonian heating on MHD flow of Casson fluid over a nonlinearly stretching sheet saturated in a porous medium." *Journal of King Saud University-Science* 29, no. 2 (2017): 250-259. https://doi.org/10.1016/j.jksus.2016.05.003

[24] Ebaid, Abdelhalim, and Mohammed A. Al Sharif. "Application of Laplace transform for the exact effect of a magnetic field on heat transfer of carbon nanotubes-suspended nanofluids." *Zeitschrift für Naturforschung A* 70, no. 6 (2015): 471-475. https://doi.org/10.1515/zna-2015-0125

[25] Saleh, Hoda, Elham Alali, and Abdelhalim Ebaid. "Medical applications for the flow of carbon-nanotubes suspended nanofluids in the presence of convective condition using Laplace transform." *Journal of the association of Arab universities for basic and applied sciences* 24, no. 1 (2017): 206-212. https://doi.org/10.1016/j.jaubas.2016.12.001

[26] Maranna, T., K. N. Sneha, U. S. Mahabaleshwar, Ioannis E. Sarris, and Theodoros E. Karakasidis. "An effect of radiation and MHD Newtonian fluid over a stretching/shrinking sheet with CNTs and mass transpiration." *Applied Sciences* 12, no. 11 (2022): 5466. https://doi.org/10.3390/app12115466

[27] Sneha, K. N., U. S. Mahabaleshwar, A. Chan, and M. Hatami. "Investigation of radiation and MHD on non-Newtonian fluid flow over a stretching/shrinking sheet with CNTs and mass transpiration." *Waves in Random and Complex Media* (2022): 1-20. https://doi.org/10.1080/17455030.2022.2029616

[28] Mahabaleshwar, U. S., K. N. Sneha, Akio Miyara, and M. Hatami. "Radiation effect on inclined MHD flow past a super-linear stretching/shrinking sheet including CNTs." *Waves in Random and Complex Media* (2022): 1-22. https://doi.org/10.1080/17455030.2022.2053238

[29] Mahabaleshwar, U. S., T. Anusha, O. Anwar Bég, Dhananjay Yadav, and Thongchai Botmart. "Impact of Navier's slip and chemical reaction on the hydromagnetic hybrid nanofluid flow and mass transfer due to porous stretching sheet." *Scientific Reports* 12, no. 1 (2022): 10451. https://doi.org/10.1038/s41598-022-14692-y

[30] Wahid, N. S., N. M. Arifin, M. Turkyilmazoglu, N. A. A. Rahmin, and M. E. H. Hafidzuddin. "Effect of magnetohydrodynamic Casson fluid flow and heat transfer past a stretching surface in porous medium with slip condition." In *Journal of Physics: Conference Series*, vol. 1366, no. 1, p. 012028. IOP Publishing, 2019. https://doi.org/10.1088/1742-6596/1366/1/012028

[31] Ahmad, Sohail, Kashif Ali, Muhammad Rizwan, and Muhammad Ashraf. "Heat and mass transfer attributes of copper–aluminum oxide hybrid nanoparticles flow through a porous medium." *Case Studies in Thermal Engineering* 25 (2021): 100932. https://doi.org/10.1016/j.csite.2021.100932

[32] Khan, Umair, A. Zaib, Ilyas Khan, Dumitru Baleanu, and Kottakkaran Sooppy Nisar. "Enhanced heat transfer in moderately ionized liquid due to hybrid MoS2/SiO2 nanofluids exposed by nonlinear radiation: Stability analysis." *Crystals* 10, no. 2 (2020): 142. https://doi.org/10.3390/cryst10020142

[33] Tiwari, Raj Kamal, and Manab Kumar Das. "Heat transfer augmentation in a two-sided lid-driven differentially heated square cavity utilizing nanofluids." *International Journal of heat and Mass transfer* 50, no. 9-10 (2007): 2002-2018. https://doi.org/10.1016/j.ijheatmasstransfer.2006.09.034

[34] Shah, Jamal, Farhad Ali, Naveed Khan, Zubair Ahmad, Saqib Murtaza, Ilyas Khan, and Omar Mahmoud. "MHD flow of time-fractional Casson nanofluid using generalized Fourier and Fick's laws over an inclined channel with applications of gold nanoparticles." *Scientific Reports* 12, no. 1 (2022): 17364. https://doi.org/10.1038/s41598-022-21006-9

[35] Veera Krishna, M. "Heat transport on steady MHD flow of copper and alumina nanofluids past a stretching porous surface." *Heat Transfer* 49, no. 3 (2020): 1374-1385. https://doi.org/10.1002/htj.21667

[36] Machrafi, Hatim. "Universal relation between the density and the viscosity of dispersions of nanoparticles and stabilized emulsions." *Nanoscale* 12, no. 28 (2020): 15081-15101. https://doi.org/10.1039/D0NR03130E